



# CHORUS

This is the accepted manuscript made available via CHORUS. The article has been published as:

## Collisions of low-energy electrons with isopropanol

M. H. F. Bettega, C. Winstead, V. McKoy, A. Jo, A. Gauf, J. Tanner, L. R. Hargreaves, and M. A. Khakoo

Phys. Rev. A **84**, 042702 — Published 5 October 2011

DOI: [10.1103/PhysRevA.84.042702](https://doi.org/10.1103/PhysRevA.84.042702)

# Collisions of Low-Energy Electrons with Isopropanol

M. H. F. Bettega

*Departamento de Física, Universidade Federal do Paraná,  
Caixa Postal 19044, 81531-990, Curitiba, Paraná, Brazil*

C. Winstead and V. McKoy

*A. A. Noyes Laboratory of Chemical Physics,  
California Institute of Technology, Pasadena, California 91125, USA*

A. Jo, A. Gauf, J. Tanner, L. R. Hargreaves, and M. A. Khakoo

*Department of Physics, California State University, Fullerton, California 92834, USA*

## Abstract

We report measured and calculated cross sections for elastic scattering of low-energy electrons by isopropanol (propan-2-ol). The experimental data were obtained using the relative flow technique with helium as the standard gas and a thin aperture as the collimating target gas source, which permits use of this method without the restrictions imposed by the relative flow pressure conditions on helium and the unknown gas. The differential cross sections were measured at energies of 1.5, 2, 3, 5, 6, 8, 10, 15, 20 and 30 eV and for scattering angles from  $10^\circ$  to  $130^\circ$ . The cross sections were computed over the same energy range employing the Schwinger multichannel method in the static-exchange plus polarization approximation. Agreement between theory and experiment is very good. The present data are compared with previous calculated and measured results for *n*-propanol, the other isomer of  $C_3H_7OH$ . Although the integral and momentum transfer cross sections for the isomers are very similar, the differential cross sections show a strong isomeric effect: in contrast to the *f*-wave behavior seen in scattering by *n*-propanol, *d*-wave behavior is observed in the cross sections of isopropanol. These results corroborate our previous observations in electron collisions with isomers of  $C_4H_9OH$ .

PACS numbers: 34.80.Bm, 34.80.Gs

## I. INTRODUCTION

Recent studies of electron collisions with methanol ( $\text{CH}_3\text{OH}$ ) and ethanol ( $\text{C}_2\text{H}_5\text{OH}$ ) [1], *n*-propanol ( $\text{C}_3\text{H}_7\text{OH}$ ) and *n*-butanol ( $\text{C}_4\text{H}_9\text{OH}$ ) [2], and the other isomers of  $\text{C}_4\text{H}_9\text{OH}$ , namely isobutanol, *t*-butanol and 2-butanol [3], show a broad structure in the elastic integral cross section (ICS) of each molecule around 10 eV. However, the differential cross sections (DCS) of the straight-chain molecules, namely ethanol, *n*-propanol, and *n*-butanol, show an *f*-wave scattering pattern between 5 to 10 eV, while branched systems such as isobutanol, *t*-butanol, and 2-butanol show a *d*-wave pattern. Similar behavior was also seen in alkanes [4–12]. These results suggest that the DCS of isopropanol (propan-2-ol or isopropyl alcohol), the branched isomer of  $\text{C}_3\text{H}_7\text{OH}$ , should also exhibit a *d*-wave pattern. To explore this question, we have carried out a joint experimental and theoretical study of elastic electron collisions with isopropanol. The differential cross sections were measured at incident energies between 1.5 and 30 eV and for scattering angles from  $10^\circ$  to  $130^\circ$  using the relative flow technique with helium as the standard gas and a thin aperture as the collimating target gas source. Calculations using the Schwinger multichannel (SMC) method in the static-exchange plus polarization (SEP) approximation were performed for the same range of energies. The influence of the long-range dipole potential on the cross sections was included in the calculations through Born closure on the scattering amplitude.

The outline of the paper is as follows. In Sec. II, the experimental setup is described, while Sec. III briefly describes the method employed in the calculations. In Sec. IV, the results are presented and discussed. The paper concludes with a brief summary of the present findings.

## II. EXPERIMENT

The experimental apparatus has been described in previous articles, e.g., Khakoo *et al.* [13], so only a brief description will be given here. The apparatus consisted of a spectrometer using crossed target and electron beams, housed in a high-vacuum chamber evacuated to a base pressure of  $\sim 2 \times 10^{-7}$  Torr by a single 10-inch diffusion pump. The electron gun and the detector employed double hemispherical energy selectors, with cylindrical lenses used to transport and focus electrons. The spectrometer was baked to about  $130^\circ\text{C}$  by magnetically free biaxial heaters (ARi Industries model BXX06B41-4K). The remnant magnetic field in

the collision region was reduced to less than 1 mG by using a double  $\mu$ -metal shield as well as a single Helmholtz coil that eliminated the vertical component of the Earth's magnetic field. The beam produced by the electron gun could be focused at electron energies down to 1.5 eV, with an energy resolution of 45–50 meV (full width at half-maximum, FWHM). Typical beam currents were around 20 nA. Over many weeks of the measurements, the spectrometer required minor periodic tuning to maintain the long-term stability of the current, which varied by no more than 10% at any time. The energy of the electron beam was established within an uncertainty of  $\pm 20$  meV by recording the beam energy required to observe the dip in the He elastic-scattering cross section due to the  $2^2S$  He $^-$  resonance. The contact potential was found to be  $0.664 \pm 0.030$  eV, determined as the difference between the observed energy of this dip and its established energy of 19.366 eV [14]. Energy-loss spectra of the elastic peak were collected at fixed incident electron energy ( $E_0$ ) values and electron scattering angles  $\theta$  by repetitive, multichannel-scaling techniques. Scattered electrons entered the analyzer and were detected by a discrete dynode electron multiplier (Equipe Thermodynamique et Plasmas model AF151). The detection efficiency of the detector remained constant for electron count rates up to 1 MHz, without saturating, while the background count rate was  $< 0.01$  Hz. The angular resolution of the electron analyzer was  $2^\circ$  FWHM.

The effusive target gas beam was formed by flowing gas through a thin aperture of 0.3 mm diameter, described previously [15]. This aperture, located 6 mm below the axis of the electron beam, was incorporated into a movable source arrangement [16]. The movable gas source method has been well tested previously [17] and enabled the expedient and accurate determination of background scattering rates. The gas needle, as well as all other metal surfaces exposed to the electron beam, were coated in soot from an acetylene flame to reduce the emission of secondary electrons. The pressures behind the source for isopropanol and helium were about 0.1 and 1.0 Torr, respectively, and the pressure in the experimental chamber was  $\sim 1 \times 10^{-6}$  Torr with the gas beam on. The gas beam temperature, determined by the apparatus temperature in the collision region, was about  $130^\circ\text{C}$ ; however, in most of the gas-handling copper tubing, the temperature was  $65^\circ\text{C}$ , with the higher temperature only in the last 4 cm of the gas handling system before the gas exited into the collision region. The gas-kinetic molecular diameter of isopropanol was determined, based on the flow-rate vs. drive pressure analysis [17], to be  $7.36 \times 10^{-8}$  cm, slightly smaller than that of *n*-propanol ( $7.49 \times 10^{-8}$  cm) at a temperature of  $74^\circ\text{C}$  [1].

Elastic scattering measurements were taken at  $E_0$  values of 1.5, 2.0, 3.0, 5.0, 6.0, 8.0, 10.0, 15, 20, and 30 eV for scattering angles ranging from  $10^\circ$  to  $130^\circ$ . Integral elastic and momentum-transfer cross sections (MTCS) were computed from the measured DCS by extrapolating the DCS to  $0^\circ$  and  $180^\circ$ , using theory as a guide where possible. At energies below 5 eV, the extrapolation to forward angles was guided using the Born-dipole form of the DCS for a dipole moment of 1.66 Debye (D) [18] and a rotational energy loss of 5 meV. Above this energy, the present calculated data were used to guide the extrapolation.

### III. THEORY

The cross section calculations were performed with the SMC method implemented for parallel computers. Both the method [19] and implementation [20] have been described in detail elsewhere, so here only those aspects which are relevant to the present study are discussed.

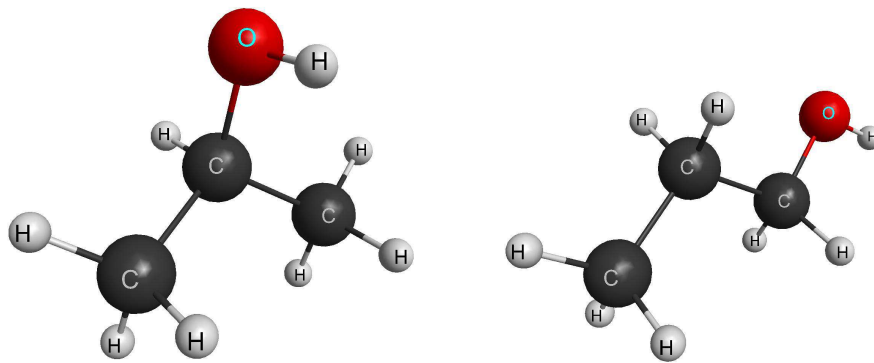


FIG. 1. (Color online) Geometrical structure of  $C_3H_7OH$  isomers. Left, isopropanol; right, *n*-propanol.

The bound-state and scattering calculations for isopropanol employed the same proce-

ture as was used for *n*-propanol [2]. The geometry of the ground state was optimized within the  $C_s$  point group using GAMESS [21] at the level of second-order Møller-Plesset perturbation theory (MP2) in the 6-31G(*d*) basis set. The resulting structure is shown in Fig. 1 (generated using MacMolPlt [22]), which also shows *n*-propanol for comparison. Although the minimum-energy conformation of gas-phase isopropanol appears to be a somewhat different  $C_1$  structure [23], based on previous results for *n*-propanol and *n*-butanol [2], it is expected that carrying out the calculations in the  $C_s$  group does not affect the cross sections significantly.

TABLE I. Symmetry groups used in our calculations, computed and experimental dipole moments  $\mu$  (Debye), and the number of CSFs per symmetry ( $A'$  and  $A''$ ) for the SEP calculations, for the two  $C_3H_7OH$  isomers.

Molecule	Group	$\mu$	$\mu_{expt}$	$A'$	$A''$
<i>n</i> -propanol	$C_s$	1.69	1.55 <sup><i>b</i></sup>	10423	10130
isopropanol	$C_s$	1.86	1.66 <sup><i>a</i></sup> ; 1.58 <sup><i>b</i></sup>	10346	10207

<sup>*a*</sup> Ref. [18]; <sup>*b*</sup> Ref. [25]

The ground-state electronic wave function at the optimized geometry was described at the Hartree-Fock level with the DZV++G(2*d*,1*p*) basis set. Scattering calculations were carried out in the SEP approximation. In the SMC method, polarization effects are taken into account through single (virtual) excitations promoting an electron from an occupied (hole) orbital of the Hartree-Fock ground state to an unoccupied (particle) orbital. These  $N$ -particle configurations are then antisymmetrized with one-particle (scattering) orbitals to construct the ( $N + 1$ )-particle basis set. Modified virtual orbitals (MVOs) [24] were employed to represent the particle and the scattering orbitals. The MVOs were generated from a cationic Fock operator with charge +6. Singlet-coupled excitations from the 10 highest hole orbitals into the 20 lowest particle (MVOs) were included, while all MVOs were used as scattering orbitals. This procedure resulted in 10 346 double configuration state functions (CSFs) for  $A'$  symmetry and 10 207 CSFs for  $A''$ , for a total of 20 553 CSFs.

The permanent dipole moment of isopropanol has been measured to be 1.66 D [18] and 1.58 D [25], similar to that of *n*-propanol (1.55 D). The present calculation yields a larger value of 1.86 D (see Table I). The long-range character of the dipole potential was accounted

for in the scattering amplitude by the standard Born closure procedure [1]. The SMC amplitude was retained up to an  $\ell_{SMC}$  ranging from 1 or 2 at low energy, to between 3 and 5 at intermediate energies, and up to 12 at higher energies. Table I shows a comparison between the symmetry group, the computed and the experimental dipole moments, and the number of CSFs used in the *n*-propanol and isopropanol calculations.

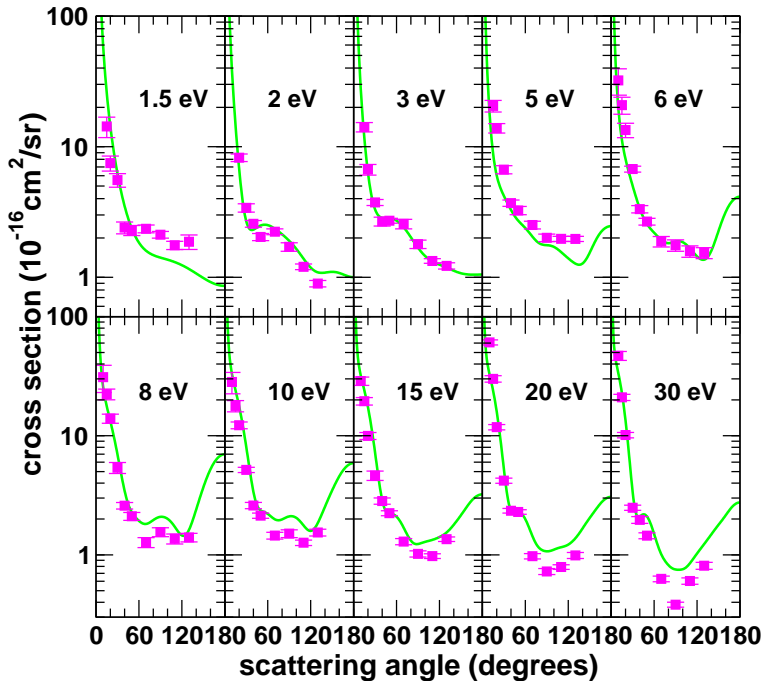


FIG. 2. (Color online) Differential cross sections for isopropanol. Solid (green) line, present computed results; squares (magenta), present experimental data.

#### IV. RESULTS AND DISCUSSION

The measured DCS and corresponding ICS and MTCS data are given in Table II, along with the experimental uncertainties. Fig. 2 compares the measured and computed DCS, which agree very well except at 20 and 30 eV, where the calculated results are larger. At these higher energies, there are many open channels, including ionization, but the present single-channel calculation does not allow flux to escape into them from the elastic channel. As expected, the long-range dipole potential dominates the low-angle scattering, leading to a sharp increase in the DCS there. Both the calculated and the measured DCS exhibit

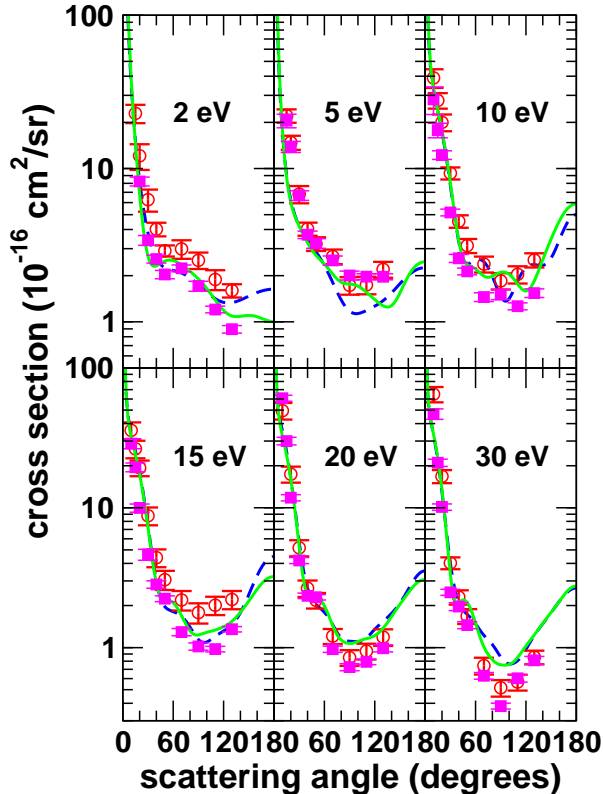


FIG. 3. (Color online) Differential cross sections for the  $C_3H_7OH$  isomers at selected energies. Solid (green) line, present computed results for isopropanol; dashed (blue) line,  $n$ -propanol; square (magenta), present experimental data for isopropanol; open circles (red) experimental data for  $n$ -propanol. The results from  $n$ -propanol were taken from Ref. [2].

clear  $d$ -wave behavior at 6, 8 and 10 eV. For comparison, Fig. 3 contrasts the DCS of isopropanol with previous results [2] for  $n$ -propanol, which displays a distinct  $f$ -wave pattern at intermediate angles. These isomeric differences are further exhibited in Fig. 4, which compares calculated DCS at 6, 7, 8, 9, and 10 eV for isopropanol,  $n$ -propanol, isobutanol,  $n$ -butanol [2], isobutane, and  $n$ -butane [2, 3, 12]. This extended comparison shows that the branched-chain molecules isopropanol, isobutane and isobutanol have a dominant  $d$ -wave scattering pattern, while their straight-chain isomers  $n$ -propanol,  $n$ -butane and  $n$ -butanol have a dominant  $f$ -wave pattern. Clearly, the arrangement of the atoms within the molecule, including the location of the hydroxyl group, affects the leading partial-wave contributions to the DCSs. We note that 2-butanol, not shown in Fig. 4, also displays the  $d$ -wave pattern of a branched system [3].

Fig. 5 shows the present calculated and measured ICS for isopropanol in comparison with



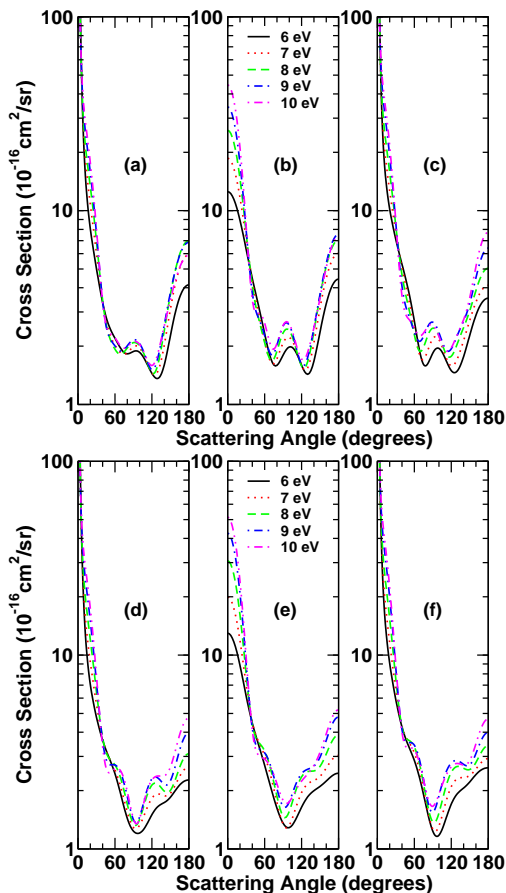


FIG. 4. (Color online) Calculated differential cross sections for (a) isopropanol, (b) isobutane, (c) isobutanol, (d) *n*-propanol, (e) *n*-butane and (f) *n*-butanol at 6, 7, 8, 9, and 10 eV. The results for isobutane and *n*-butane are from Ref. [12], those for isobutanol, from Ref. [3], and those for *n*-butanol from Ref. [2]. See text for discussion.

our previous results for *n*-propanol [2]. The cross sections of the two isomers are similar at all energies. Agreement between the calculated and experimental ICS for isopropanol is good, though not as good as for *n*-propanol [2], with the calculated cross sections lying inside the error bars at all energies. The main feature in the ICS is a broad maximum at around 10 eV. Similar structures are present in the ICS of methanol, ethanol, *n*-propanol, and the isomers of butanol [1–3], but also in the ICS of alkanes and alkenes, suggesting an association with short-lived C–H and/or C–C  $\sigma^*$  resonances rather than a specific connection to the alcohols. The MTCS for isopropanol is shown in Fig. 6, together with previous theoretical and experimental data for *n*-propanol [2]. A broad maximum near 10 eV is again evident and the MTCS of the two isomers are again similar.

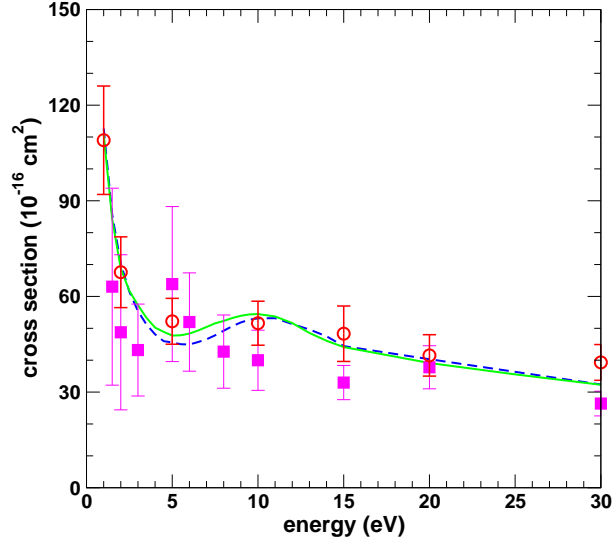


FIG. 5. (Color online) Integral cross sections for the  $\text{C}_3\text{H}_7\text{OH}$  isomers. Solid (green) line, present computed results for isopropanol; dashed (blue) line,  $n$ -propanol; square (magenta), present experimental data for isopropanol; open circles (red) experimental data for  $n$ -propanol. The results from  $n$ -propanol were taken from Ref. [2].

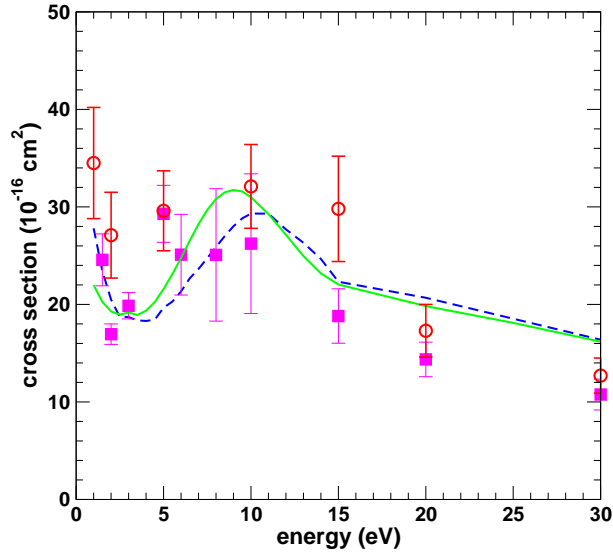


FIG. 6. (Color online) Momentum transfer cross sections for the  $\text{C}_3\text{H}_7\text{OH}$  isomers. Solid (green) line, present computed results for isopropanol; dashed (blue) line,  $n$ -propanol; square (magenta), present experimental data for isopropanol; open circles (red) experimental data for  $n$ -propanol. The results from  $n$ -propanol were taken from Ref. [2].

## V. SUMMARY

Measured and computed elastic differential, integral, and momentum-transfer cross sections have been presented for electron collisions with isopropanol at energies from 1.5 to 30 eV. Good agreement is found between the experimental and theoretical results. While the integral and momentum-transfer cross sections of isopropanol and *n*-propanol are similar in magnitude and both show a broad maximum near 10 eV, the differential cross sections are distinct, with isopropanol showing predominantly *d*-wave and *n*-propanol predominantly *f*-wave character in the  $\sim 6$ –10 eV range. Similar behavior was observed for the isomers of C<sub>4</sub>H<sub>9</sub>OH and has also been seen in scattering by linear and branched alkanes [3].

Because the *d*- or *f*-wave scattering behavior is observed in gases at or above room temperature, which may contain more than one conformer, and because calculations that assume non-optimal conformers having *C<sub>s</sub>* symmetry agree well with the measurements, the scattering pattern appears to depend only on the general arrangement of the atoms in the molecule (i.e., straight vs. branched chains) and not on conformational details such as the orientation of the hydrogens within CH<sub>3</sub> or OH groups. It is also remarkable that (with the exception of methanol) each alcohol should have the same scattering behavior as the alkane obtained by replacing the polar OH group with a nonpolar CH<sub>3</sub> group. Whether the same holds true for the NH<sub>2</sub> and F groups that are also isoelectronic with OH remains to be determined, as existing electron scattering data for aminoalkanes and monofluoroalkanes are quite limited.

## ACKNOWLEDGMENTS

This work was funded through a collaborative program by the U.S. National Science Foundation under Grants PHY 0653452 and PHY 0653396 and by the Brazilian Conselho Nacional de Desenvolvimento Científico e Tecnológico (CNPq) under Project 490415-2007-5. M.H.F.B. also acknowledges support from the Paraná state agency Fundação Araucária and from FINEP (under Project no. CT-Infra), as well as computational support from Professor Carlos M. de Carvalho at DFis-UFPR and at LCPAD-UFPR. Work by V.M. and C.W. was also supported by the Chemical Sciences, Geosciences, and Biosciences Division, Office of Basic Energy Sciences, Office of Science, U.S. Department of Energy. The authors

acknowledge the use of the Jet Propulsion Laboratory's Supercomputing and Visualization Facility, where the present calculations were performed.

- 
- [1] M. A. Khakoo, J. Blumer, K. Keane, C. Campbell, H. Silva, M. C. A. Lopes, C. Winstead, V. McKoy, R. F. da Costa, L. G. Ferreira, M. A. P. Lima, and M. H. F. Bettega, *Phys. Rev. A* **77**, 042705 (2008).
  - [2] M. A. Khakoo, J. Muse, H. Silva, M. C. A. Lopes, C. Winstead, V. McKoy, E. M. de Oliveira, R. F. da Costa, M. T. do N. Varella, M. H. F. Bettega, and M. A. P. Lima, *Phys. Rev. A* **78**, 062714 (2008).
  - [3] M. H. F. Bettega, C. Winstead, and V. McKoy, *Phys. Rev. A* **82**, 062709 (2010).
  - [4] D. Matsunaga, M. Kubo, and H. Tanaka, in *Proceedings of the 12<sup>th</sup> International Conference on the Physics of Electronic and Atomic Collisions*, S. Datz, editor (North-Holland, Amsterdam, 1981), p. 358.
  - [5] P. J. Curry, W. R. Newell, and A. C. H. Smith, *J. Phys. B* **18**, 2303 (1985).
  - [6] H. Tanaka, L. Boesten, D. Matsunaga, and T. Kudo, *J. Phys. B* **21**, 1255 (1988).
  - [7] W. Sun, C. W. McCurdy, and B. H. Lengsfeld III, *J. Chem. Phys.* **97**, 5480 (1992).
  - [8] L. Boesten, M. A. Dillon, H. Tanaka, M. Kimura, and H. Sato, *J. Phys. B* **27**, 1845 (1994).
  - [9] M. H. F. Bettega, R. F. da Costa, and M. A. P. Lima, *Phys. Rev. A* **77**, 052706 (2008).
  - [10] M. H. F. Bettega, R. F. da Costa e M. A. P. Lima, *Braz. J. Phys.* **39**, 68 (2009).
  - [11] A. R. Lopes, M. H. F. Bettega, M. A. P. Lima, and L. G. Ferreira, *J. Phys. B* **37**, 997 (2004).
  - [12] M. H. F. Bettega, M. A. P. Lima, and L. G. Ferreira, *J. Phys. B* **40**, 3015 (2007).
  - [13] M. A. Khakoo, C. E. Beckmann, S. Trajmar, and G. Csanak, *J. Phys. B* **27**, 3159 (1994).
  - [14] J. H. Brunt, G. C. King, and F. H. Read, *J. Phys. B* **10**, 1289 (1977).
  - [15] M. A. Khakoo, H. Silva, J. Muse, M. C. A. Lopes, C. Winstead, and V. McKoy, *Phys. Rev. A* **78**, 052710 (2008).
  - [16] M. Hughes, K. E. James, Jr., J. G. Childers, and M. A. Khakoo, *Meas. Sci. Technol.* **14**, 841 (1994).
  - [17] M. A. Khakoo, K. Keane, C. Campbell, N. Guzman and K. Hazlett, *J. Phys. B* **40**, 3601 (2007).
  - [18] Handbook of Chemistry and Physics, CRC Press, Inc. Boca Raton, Florida, USA, 64th Edi-

- tion, E-59 (1983).
- [19] K. Takatsuka and V. McKoy, Phys. Rev. A **24**, 2473 (1981); K. Takatsuka and V. McKoy, Phys. Rev. A **30**, 1734 (1984).
- [20] C. Winstead and V. McKoy, Comput. Phys. Commun. **128**, 386 (2000).
- [21] M. W. Schmidt, K. K. Baldrige, J. A. Boatz, S. T. Elbert, M. S. Gordon, J. H. Jensen, S. Koseki, N. Matsunaga, K. A. Nguyen, S. J. Su, T. L. Windus, M. Dupuis, and J. A. Montgomery, J. Comput. Chem. **14**, 1347 (1993).
- [22] B. M. Bode and M. S. Gordon, J. Mol. Graphics Mod. **16**, 133 (1998).
- [23] E. Hirota, J. Phys. Chem. **83**, 1457 (1979).
- [24] C. W. Bauschlicher, J. Chem. Phys. **72**, 880 (1980).
- [25] <http://cccbdb.nist.gov/default.htm>

TABLE II. Measured differential cross sections ( $10^{-16}$  cm<sup>2</sup> / sr ) for elastic electron scattering by isopropanol. The second column at each energy lists the error estimate. The entries in italic are extrapolated values used in computing the integral elastic  $\sigma_I$  and momentum-transfer  $\sigma_{MT}$  cross sections, which are listed, along with their error estimates, at the foot of the columns. The notation  $[n]$  signifies  $10^n$ .

$\theta$ (deg)	1.5eV	2eV	3eV	5eV	6eV	8eV	10eV	15eV	20eV	30eV										
0	<i>6.12[5]</i>	<i>8.17[5]</i>	<i>1.23[6]</i>	<i>3.75[5]</i>	<i>2.53[5]</i>	<i>1.34[5]</i>	<i>8.93[4]</i>	<i>5.95[4]</i>	<i>8.93[4]</i>	<i>4.17[4]</i>										
1	<i>4.71[3]</i>	<i>3.54[3]</i>	<i>2.37[3]</i>	<i>3.75[3]</i>	<i>2.54[3]</i>	<i>1.36[3]</i>	<i>9.20[2]</i>	<i>6.25[2]</i>	<i>9.61[2]</i>	<i>4.72[2]</i>										
3	<i>527</i>	<i>395</i>	<i>264</i>	<i>416</i>	<i>289</i>	<i>168</i>	<i>127</i>	<i>96.1</i>	<i>167</i>	<i>101</i>										
5	<i>190</i>	<i>142</i>	<i>94.9</i>	<i>149</i>	<i>110</i>	<i>72.2</i>	<i>62.5</i>	<i>53.1</i>	<i>101</i>	<i>68.9</i>										
8	<i>74.2</i>	<i>55.7</i>	<i>37.1</i>	<i>58.5</i>	<i>47.8</i>	<i>38.9</i>	<i>39.3</i>	<i>36.9</i>	<i>74.8</i>	<i>53.6</i>										
10	<i>47.6</i>	<i>35.7</i>	<i>23.8</i>	<i>37.9</i>	32.2	7.34	31.0	7.98	28.3	5.76	28.8	2.32	60.8	2.98	47.0	4.04				
15	14.3	2.55	<i>15.9</i>	14.1	1.16	20.5	2.08	20.8	3.09	22.3	2.32	17.8	1.93	19.5	1.41	30.0	1.86	21.0	1.26	
20	7.49	0.99	8.24	0.55	6.68	0.62	13.9	1.15	13.4	1.69	14.0	1.22	12.3	0.80	9.97	0.67	11.8	0.61	10.1	0.53
30	5.55	0.66	3.40	0.25	3.75	0.20	6.68	0.48	6.74	0.35	5.39	0.57	5.17	0.26	4.63	0.42	4.20	0.21	2.49	0.12
40	2.40	0.25	2.57	0.15	2.68	0.21	3.70	0.21	3.33	0.21	2.59	0.16	2.60	0.16	2.83	0.17	2.35	0.10	1.97	0.13
50	2.29	0.20	2.04	0.13	2.71	0.12	3.25	0.24	2.67	0.16	2.11	0.16	2.13	0.11	2.24	0.11	2.29	0.10	1.45	0.08
70	2.35	0.16	2.23	0.12	2.56	0.21	2.52	0.17	1.88	0.17	1.27	0.12	1.45	0.09	1.29	0.08	0.97	0.05	0.63	0.03
90	2.12	0.12	1.71	0.13	1.79	0.13	2.01	0.13	1.76	0.18	1.55	0.13	1.51	0.11	1.02	0.06	0.73	0.04	0.38	0.02
110	1.76	0.13	1.20	0.06	1.33	0.05	1.97	0.09	1.58	0.16	1.37	0.13	1.26	0.07	0.98	0.04	0.79	0.04	0.60	0.04
130	1.87	0.24	0.90	0.05	1.22	0.07	1.97	0.09	1.54	0.15	1.40	0.12	1.54	0.10	1.35	0.06	0.99	0.06	0.81	0.05
140	<i>1.85</i>	<i>0.88</i>	<i>1.20</i>	<i>2.01</i>	<i>1.63</i>	<i>2.02</i>	<i>2.54</i>	<i>1.70</i>	<i>1.17</i>	<i>1.00</i>										
150	<i>1.70</i>	<i>0.89</i>	<i>1.15</i>	<i>2.43</i>	<i>2.31</i>	<i>3.10</i>	<i>3.47</i>	<i>2.04</i>	<i>1.43</i>	<i>1.20</i>										
160	<i>1.50</i>	<i>0.87</i>	<i>1.10</i>	<i>3.14</i>	<i>3.22</i>	<i>4.39</i>	<i>4.57</i>	<i>2.49</i>	<i>1.73</i>	<i>1.44</i>										
170	<i>1.30</i>	<i>0.83</i>	<i>1.05</i>	<i>3.70</i>	<i>3.96</i>	<i>5.46</i>	<i>5.51</i>	<i>2.90</i>	<i>2.03</i>	<i>1.72</i>										
180	<i>1.10</i>	<i>0.81</i>	<i>1.05</i>	<i>3.88</i>	<i>4.22</i>	<i>5.87</i>	<i>5.89</i>	<i>3.06</i>	<i>2.15</i>	<i>1.85</i>										
$\sigma_I$	63.1	30.9	48.7	24.3	43.2	14.4	63.9	24.3	52.0	15.4	42.7	11.5	40.0	9.44	33.0	5.36	37.8	6.76	26.4	3.87
$\sigma_{MT}$	24.6	2.66	17.0	1.05	19.9	1.35	29.3	2.92	25.1	4.14	25.1	6.79	26.2	7.16	18.8	2.79	14.4	1.77	10.8	1.58